Original Research

Optical imaging of mitochondrial redox state in rodent models with 3-iodothyronamine

Zahra Ghanian[1], Sepideh Maleki[1], Hannah Reiland[2], Daniel E Bütz[3], Grazia Chiellini[2], Fariba-Assadi Porter[2,4] and Mahsa Ranji[1]

[1]Biophotonics Laboratory, Department of Electrical Engineering and Computer Science, University of Wisconsin Milwaukee, Milwaukee, WI 53211-3029, USA; [2]Department of Biochemistry, University of Wisconsin Madison, WI 53706, USA; [3]Department of Animal Sciences, University of Wisconsin Madison, WI 53706, USA; [4]NMR Facility at Madison, University of Wisconsin Madison, WI 53706, USA
Corresponding author: Mahsa Ranji. Email: ranji@uwm.edu

Abstract

This study used an optical technique to measure the effects of treating low (10 mg/kg) and high (25 mg/kg) doses of 3-iodothyronamine (T_1AM) on the metabolism in the kidney and heart of mice. The ratio of two intrinsic fluorophores in tissue, (NADH/FAD), called the NADH redox ratio (NADH RR), is a marker of the metabolic state of the tissue. A cryofluorescence imaging instrument was used to provide a quantitative assessment of NADH RR in both kidneys and hearts in mice treated with 3-iodothyronamine. We compared those results to corresponding tissues in control mice. In the kidneys of mice treated with a high dose T_1AM, the mean values of the maximum projection of NADH RR were 2.6 ± 0.6 compared to 3.20 ± 0.03 in control mice, indicating a 19% (± 0.4) significant increase in oxidative stress (OS) in the high dose-treated kidneys ($P = 0.047$). However, kidneys treated with a low dose of T_1AM showed no difference in NADH RR compared to the kidneys of control mice. Furthermore, low versus high dose treatment of T_1AM showed different responses in the heart than in the kidneys. The mean value of the maximum projection of NADH RR in the heart changed from 3.0 ± 0.3 to 3.2 ± 0.6 for the low dose and the high dose T_1AM-treated mice, respectively, as compared to 2.8 ± 0.7 in control mice. These values correspond to a 9% (± 0.5) ($P = 0.045$) and 14% (± 0.5) ($P = 0.008$) significant increase in NADH RR in the T_1AM-treated hearts, indicating that the high dose T_1AM-treated tissues have reduced OS compared to the low dose-treated tissues or the control tissues. These results suggest that while T_1AM at a high dose increases oxidative response in kidneys, it has a protective effect in the heart and may exert its effect through alternative pathways at different doses and at tissue specific levels.

Keywords: 3-Iodothyronamine, optical imaging, NADH, FAD, mitochondrial redox ratio, oxidative stress

***Experimental Biology and Medicine* 2014; 239: 151–158. DOI: 10.1177/1535370213510252**

Introduction

3-Iodotyhronamine (T_1AM) is an endogenous thyroid hormone (TH) derivative regarded as a rapid modulator of behavior and metabolism.[1] Administration of exogenous T_1AM produces functional effects that show a rapid onset and are often opposite to those induced by TH.[1–3] In rodents, an intraperitoneal T_1AM injection rapidly induces hypothermia, decreases cardiac function, and decreases the respiratory quotient suggesting a shift from primarily carbohydrate to predominantly lipid utilization.[1,2,4] Recent results from NMR-based metabolomics and breath studies have shown that chronic T_1AM exposure induces a rapid increase in lipid mobilization, followed by increased protein breakdown after a few days. T_1AM-treated mice show continual reduction in body weight independent of food consumption, and only regain 1.8% of the lost weight in the two weeks following T_1AM withdrawal. Intracerebroventricular (ICV) injection of T_1AM modifies hormone secretion, food intake, and memory acquisition.[5] Among its metabolic effects, T_1AM has been reported to produce hyperglycaemia.[6] Notably, hyperglycaemia occurs after administration of relatively low doses of exogenous T_1AM, producing changes in tissue concentration of about one order of magnitude.[5] In addition, a clinical investigation performed in a small series of patients revealed that serum T_1AM concentration was significantly correlated with glycated hemoglobin, and significantly increased in a subgroup of diabetic patients.[7] Therefore, the effects of T_1AM on glucose metabolism might have physiological and pathophysiological relevance. Hyperglycaemia, which occurs during type 2 diabetes, causes disorders of

the oxidative–antioxidative balance in cells leading to increased free-radical formation and induction of OS.[8]

Optical fluorescence techniques have been shown to have a high sensitivity and specificity for discriminating between diseased and non-diseased tissue. Fluorescence imaging provides specific information on intrinsic fluorophores in tissue as a diagnostic tool for early detection of different diseases.[9–13] Mitochondrial metabolic coenzymes such as nicotinamide adenine dinucleotide (NADH) and flavoprotein adenine dinucleotide ($FADH_2$) are the primary electron carriers in oxidative phosphorylation.[14] NADH and FAD (the oxidized form of $FADH_2$) are autofluorescent and can be monitored without exogenous labels through the use of optical techniques. These coenzymes are beneficial in that NADH is primarily fluorescent in its reduced biochemical state, whereas FAD is only fluorescent in its oxidized form. Therefore, we can probe the oxidative state of the metabolism in tissue by imaging these two coenzymes. The fluorescent signals of these intrinsic fluorophores have been used as indicators of tissue metabolism in injury due to hypoxia,[11,12,15] hyperoxia,[13,16] ischemia-reperfusion,[11,12] and diabetes[17] and also as indicators for the response of different treatments such as photodynamic therapy[18] and cancer therapy[19–21]. Our group has recently studied other organs such as lungs and hearts in the injury models such as ischemia-reperfusion and hyperoxia,[13,15,16] as well as kidneys in diabetic nephropathy models[22] and shown that NADH RR is a prominent indicator of OS.

Our studies have demonstrated that the ratio of these fluorophores, (NADH/FAD), called the NADH redox ratio (NADH RR), acts as a quantitative marker of the mitochondrial redox and metabolic state of tissue *ex vivo*[23] and *in vivo*.[24] In this study, we applied optical fluorescence imaging to evaluate the mitochondrial redox state of two different organs, kidney and heart, from treated mice with high (25 mg/kg) and low (10 mg/kg) doses of T_1AM compared to control mice. We hypothesized that there would be a significant difference in the optical redox ratio of high dose-treated organs in comparison to corresponding organs in control mice.

Although the molecular mechanisms and associated metabolic pathways of T_1AM are not well understood, there is evidence that exogenous application of T_1AM results in different uptake levels and accumulations in a tissue-specific manner.[25] Chiellini et al.[25] recently reported that while T_1AM is initially distributed in specific tissues such as kidney, liver, gallbladder, stomach, and intestine, after 24 h a majority of this chemical messenger is only found in the liver, adipose tissue, and muscle. In this study, we investigated the metabolic effects of T_1AM in hearts and kidneys, two of the most metabolically active organs in the body. T_1AM treatment has two different effects on these organs and these organs also have the highest mitochondrial density, 22.8 ± 4.7 and 18.7, respectively.[17] Thus, we expect the heart and kidneys to show strong fluorescence signals from the mitochondrial coenzymes NADH and FAD, which are used to calculate the NADH RR and provide an accurate quantitative assessment of the effect of T_1AM treatment on the redox state.

Materials and Methods

Animal treatment, solution preparation, and tissue preparation

The College of Letters and Sciences Animal Care and Use Committee at the University of Wisconsin-Madison approved all animal procedures. Outbred female CD-1, *Mus musculus* mice obtained from Harlan Laboratories (Indianapolis, IN) weighing at least 35 g were maintained on a 12 h light/dark cycle and allowed *ad libitum* access to food and water. In the week prior to sacrifice, mice were given daily intraperitoneal injections of either 10 mg/kg T_1AM, 25 mg/kg T_1AM or vehicle ($n = 4$ per group). A stock solution of T_1AM (0.5 mg/μL) was prepared by solubilizing 75 mg of T_1AM into 150 μL of DMSO. The T_1AM injection solutions (10 mg/kg and 25 mg/kg) were prepared by adding 1 μL and 2.5 μL, respectively, of T_1AM stock solution to 6.0 mL of normal sterile saline. The vehicle injection was prepared in the same way without the addition of T_1AM. The final injection volume was 6 μL per gram body weight. At the time of the sacrifice, the mice were deeply anesthetized with 2.5% isofluorane for 10 min and exsanguinated. Since both control and treated tissues (kidneys and hearts) are treated identically, any 'preconditioning' effects of anaesthesia are minimized.

Freezing and embedding

The mouse kidneys and hearts were flash frozen in liquid nitrogen and kept frozen at −80°C until used for low temperature cryoimaging (−15°C). For fluorescence imaging, the tissue was embedded in a customized black mounting medium (that is not fluorescent in the excitation wavelengths) and placed on a chilled aluminium plate to immobilize it for freezing and slicing. The embedding process consists of freezing some medium as a base, embedding the tissue on the base, and then fixing its position by adding black medium around the tissue.

After embedding, the tissue was stored in an ultra low freezer (−80°C) for subsequent imaging. The plate was then installed in the cryoimager where the surface of the black medium is parallel to a microtome.

Imaging calibration

A calibration method was designed to compensate for day-to-day variation of light intensity and non-uniformity of the illumination pattern. At the beginning of each experiment and before slicing the tissue, a uniform fluorescent flat plate was placed in the same position as the tissue and imaged in the NADH and FAD channels to acquire the illumination pattern. Since the standard flat plate is fluorescent in both the NADH and FAD channels, it can account for day-to-day variations in both channels. The intensity of each channel was normalized by dividing it by the intensity of the appropriate standard flat plate captured immediately before imaging the sample.

Cryoimager

The cryoimager is an automated image acquisition and analysis system consisting of software and hardware designed to acquire fluorescence images of tissue sections. Details of this instrument have been previously reported.[26] For this study, we used a resolution of 30 μm in the *z*-direction, which resulted in approximately 250 slices per organ.

Image processing

NADH and FAD autofluorescence images from each group of tissues were processed using MATLAB. Composite images were created using all the image slices for each tissue, for both NADH and FAD signals. The ratio of NADH and FAD was calculated voxel by voxel, using MATLAB, according to equation (1):

$$\text{NADH redox ratio} = RR = NADH/FAD \qquad (1)$$

The 2-D representation of each tissue was then calculated using the maximum intensities along the *z*-axis of the NADH redox 3-D volume (maximum projection). In the maximum projection method, first a full 3D volume of images was obtained, including RR, then the maximum projection on the volumetric data was performed and the histograms were plotted for this maximum projection. The maximum projection is used since the entirety of the anatomy has a significant contribution in this representation. A histogram of the maximum projection of RR values for each group was created, and the mean (or first moment) of this histogram was calculated according to equation (2).

$$Mean = \frac{1}{N_x \times N_y} \sum_{i=1}^{N_x} \sum_{j=1}^{N_y} tissue\_Maxpro(i,j) \qquad (2)$$

where N_x and N_y are the number of pixels in the x and y directions and the pixel size in both x and y is 10 μm. The previously mentioned histograms were calculated for quantitative comparison between control and treated groups. NADH RR shows an inverse relation with the OS level of the tissue. Therefore, a higher mean value of NADH RR shows less oxidation and a smaller value of NADH RR indicates a higher level of oxidative stress (OS).

Statistical evaluation of data

Statistical analysis was carried out for the high dose-treated kidneys and hearts versus untreated control tissues using a two-tailed Student's *t*-test with $P < 0.05$ as the criterion for statistical significance.

Results

In the present study, we used the cryo-fluorescence redox imaging method to quantify the mitochondrial redox state of kidneys and hearts in mice treated with T_1AM and compared it with the corresponding untreated control tissues. Furthermore, the T_1AM-treated mice consisted of a low dose group and a high dose group. These tissue groups allowed us to investigate the effects of T_1AM on kidneys and hearts, in addition to studying the effects of the two dose levels on these tissues.

Figure 1 shows the maximum projection images of NADH, FAD, and NADH RR for a representative *kidney* from each of the three groups: the control, the low dose, and the high dose T_1AM-treated groups. First, the images show a significant decrease in the mean NADH RR of kidneys from the high dose T_1AM-treated versus the control group. Kidneys of the high dose-treated group (Figure 1, right panel) show a significant decrease in the concentration of NADH but only a small increase in FAD concentration, resulting in a lower NADH RR in these tissues as compared to the control (Figure 1, left panel). Second, the high dose-treated group shows a lower level of NADH RR in kidneys as compared to the low dose-treated (Figure 1, middle panel) kidneys. Cross sections from the high dose T_1AM-treated kidneys consistently demonstrate increased OS (Figure 1, right panel), whereas the kidneys from the low dose-treated mice (Figure 1, middle panel) do not show any change in the mitochondrial redox state as compared to the control group (Figure 1, left panel). The NADH redox histograms of Figure 1 are shown for the control (blue histogram), the low dose T_1AM-treated (green histogram), and the high dose T_1AM-treated (red histogram) groups. The histogram of the low dose-treated group is totally overlapping with the histogram of the control group, with the mean value of NADH RR for these two groups equal to 3.2 in both cases. In the high dose-treated group, the NADH RR indicates a more oxidized mitochondrial redox state with a mean value of 2.6 (2.6 ± 0.6) compared with a higher mean value of 3.2 (3.2 ± 0.03) in control kidney tissues. There is a blue shift in the histograms from the high dose T_1AM treated kidneys versus control kidneys, and the NADH redox histogram shows a 19% (±0.4) increase of oxidation in the respiratory chain in the high dose-treated group compared to control ($P = 0.047$).

Figure 2 shows an average of 9% (±0.5) and 14% (±0.5) increase in the mean NADH RR of representative *hearts* from low dose and high dose T_1AM-treated groups ($P = 0.045$ and 0.008, respectively), as compared to the control group. Hearts from the low dose and the high dose treated groups (Figure 2, middle and right panels) show a higher concentration of NADH but a lower concentration of FAD as compared to the control group (Figure 2, left panel). Hence, the NADH RR is higher in heart tissues from the treated group compared to the control group. In addition, histograms of the NADH redox from the representative heart tissue in each of the treated and control groups indicate a less oxidized mitochondrial redox state with a mean value of 3.2 (3.2 ± 0.6) for the high dose and 3.0 (3.0 ± 0.3) for the low dose-treated group compared with a lower mean value of 2.8 (2.8 ± 0.7) in the control group. This red shift in histograms in tissues from T_1AM treated mice versus control mice shows 14% (±0.5) less oxidation in the respiratory chain of hearts in the higher dose-treated group.

Figures 3 and 4 compare the mean values of histograms of maximum projected images from the control and high dose-treated kidneys and hearts, respectively. The results show a significant difference ($P = 0.047$) between high

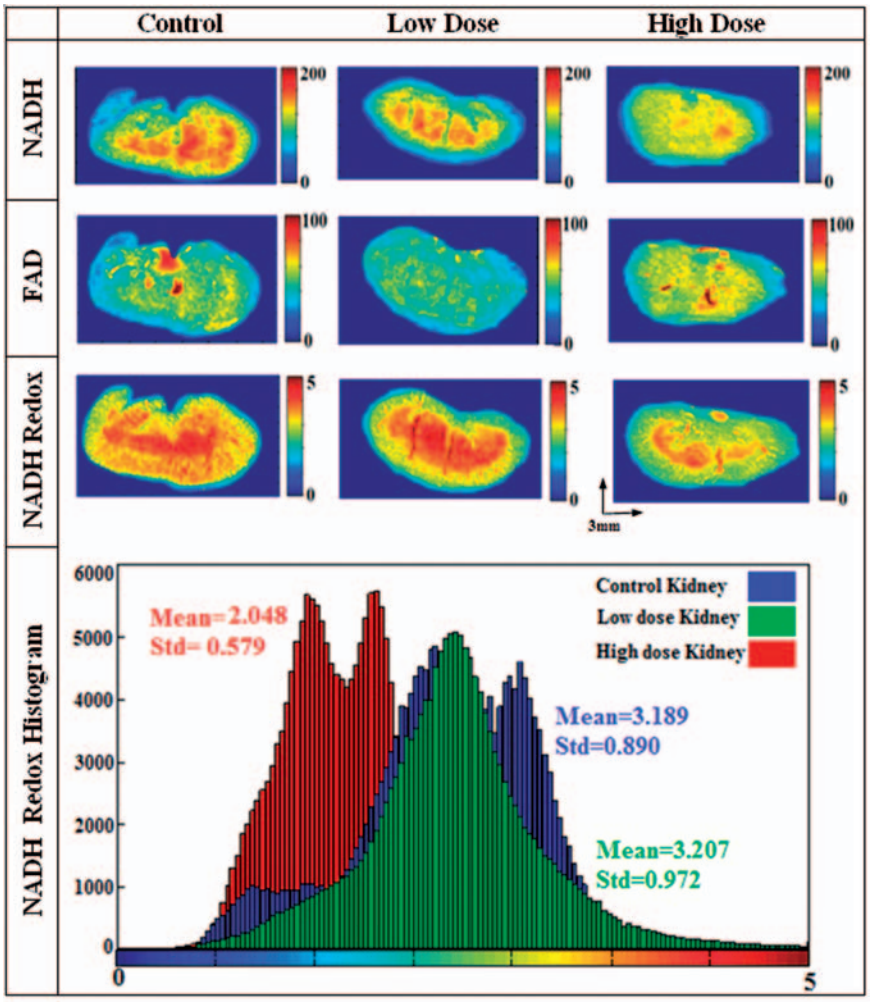

Figure 1 Representative max projected NADH, FAD and RR images and histograms comparing Redox Ratio intensity for kidneys from control, low, and high T_1AM-treated groups. Colours blue to red indicate arbitrary normalized levels of redox states from 0 to 5, NADH from 0 to 200 and FAD between 0 and 100 from minimum to maximum intensity levels. Only the NADH redox histogram of the high dose-treated (red histogram) group shows significantly more oxidation as compared to the control (blue histogram) and the low dose (green histogram) groups. Mean values of these histograms were calculated according to equation (2). (A color version of this figure is available in the online journal)

dose-treated kidneys versus the control kidneys, but the difference is not significant ($P = 0.18$) between treated and control hearts ($n = 4$ in each group).

Discussion and conclusion

The metabolic state of a cell is revealed by mitochondrial oxidative function. Mitochondrial oxidative metabolism is an important biomarker for the diagnosis and treatment of many disease pathologies, including cancer, neurodegenerative diseases,[27,28] as well as endocrine disorders, including thyroid dysfunctions[29] and diabetes.[8] The results of the present study demonstrate the utility of the cryo-fluorescence imaging method for investigating the mitochondrial redox state of kidneys and heart in response to low and high doses (10 and 25 mg/kg) of T_1AM. This method detects changes in the oxidation state of the mitochondrial respiratory chain by using NADH RR as a quantitative marker to evaluate OS in treated and control tissues.

T_1AM is an endogenous primary amine, structurally related to the TH, which produces profound metabolic effects. Endogenously produced T_1AM has been detected *in vivo* at nanomolar concentrations in several rat tissues, mouse brain, as well as in human, rat, mouse, and guinea pig blood.[30] The physiological role of T_1AM is still under investigation, and recent data suggest that it may have metabolic and endocrine effects.[31] Different pharmacological responses have been elicited after administration of exogenous T_1AM. Acute administration of T_1AM rapidly induces hypothermia, bradycardia, and hyperglycaemia in rodents. In addition, in Siberian hamsters, a hibernating rodent, as well as mice, acute high-dose T_1AM induces a profound fuelling shift away from carbohydrates and towards fat burning.[4] In the Siberian hamsters, this fuelling change is characterized by a change in respiratory quotient (RQ) from normal value of 0.9 to 0.7 that persists for 48 h after a single dose of T_1AM.[4] We have recently found that daily dosing of T_1AM (10 mg/kg/day) for two weeks leads to significant weight loss in diet-induced obese mice. Taken

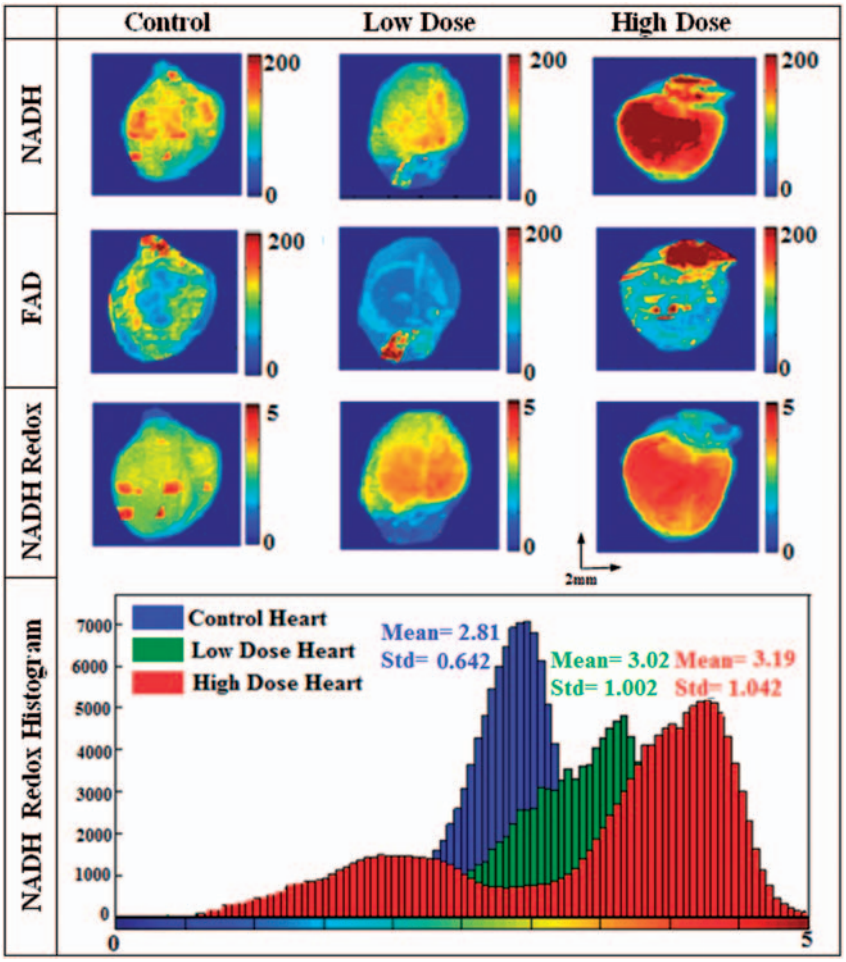

Figure 2 Representative max projected NADH, FAD and RR images and histograms comparing Redox Ratio intensity for hearts from control and T_1AM treated groups. Colours blue to red indicate arbitrary normalized levels of redox states from 0 to 5, NADH and FAD from 0 to 200 from minimum to maximum intensity levels. Oxidative stress causes less oxidation in the NADH redox histogram of both the low dose- (green histogram) and high dose-treated groups (red histogram) as compared to control (blue histogram) group. Mean values of these histograms were calculated according to equation (2). (A color version of this figure is available in the online journal)

together, all these findings provide evidence that T_1AM may have great potential as a drug for the treatment of obesity and body weight management. Therefore, in order to develop T_1AM as a drug for weight loss, it is critical to gain a better understanding of its metabolic actions and the pathways affected. The present study allowed us to quantify NADH RR signals as a marker for the energy metabolism pathway via NADH/FADH2/ATP production and to follow changes in the rate of metabolism in the kidneys and heart of animals treated with T_1AM.

Recent findings indicate that exogenously administered T_1AM was taken up by virtually every mouse tissue, with the highest concentrations detected in the liver, kidney, and gastrointestinal tract suggesting biliary and urinary excretion associated with long term liver storage.[3] As a result, we expected a higher change in the T_1AM treated mitochondrial oxidative state in the kidneys than in the heart.

In isolated hearts, exogenously administered T_1AM decreased cardiac contractility[2] and increased the resistance to ischemic injury.[32] Cardio protection occurs at T_1AM concentrations much lower than those able to affect contractile function, and is probably linked to modulation of mitochondrial permeability transition and/or ischemic arrest time.[32] A recent study revealed that mitochondrial F_1F_o-ATP synthase, the enzyme that catalyzes the phosphorylation of ADP to ATP at the expense of a proton-motive force generated by the electron transport chain in energy transducing membranes,[33] is an additional molecular target of T_1AM.[34] Interestingly, when applied to heart-derived cells, T_1AM elicited a twofold effect on activation of the F_1F_o-ATP synthase at low nanomolar concentrations, whereas it resulted an inhibition of enzymatic activity at higher concentrations, thereby affecting cell bioenergetics.

Previously, it was also proposed that the mitochondrion is the main target for other TH derivatives such as the diiodothyronines. The inner membrane of rat liver mitochondria contains iodothyronine-binding sites, showing the greatest affinity for 3,5-diiodothyronine (3,5-T2) and 3,3′-diiodothyronine (3,3′-T2).[35] The administration of such substances to hypothyroid rats stimulates liver mitochondrial respiration.[36] However, *in vitro* addition of T_1AM at low nanomolar concentration produces an inhibitory effect,[37]

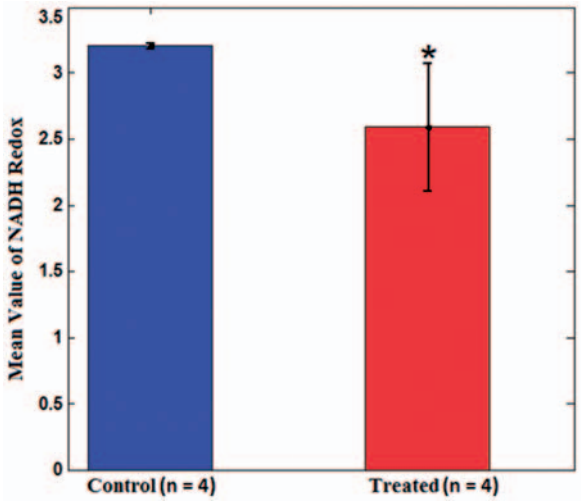

Figure 3 Bar graph plot comparing the mean values of the histograms of max projected images from kidneys obtained from control and high dose T_1AM-treated mice. The results show a significant difference between control and treated kidneys (*indicates $P = 0.047$, $n = 4$). Error bars: SEM; P values were obtained from two-tailed Student's t-test. (A color version of this figure is available in the online journal)

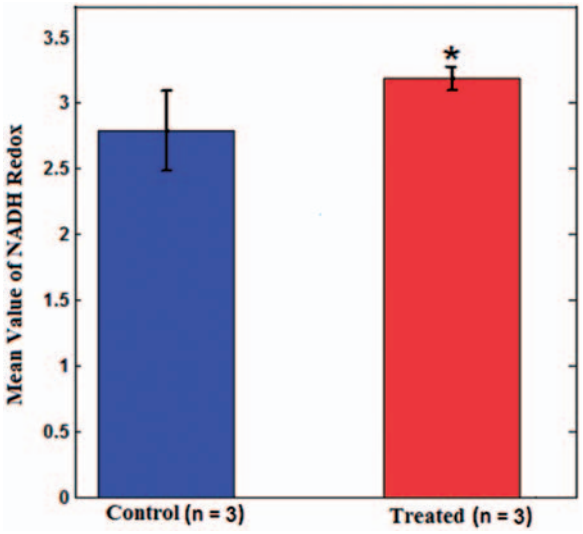

Figure 4 Bar graph plot comparing the mean values of the histograms of max projected images from hearts obtained from control and high dose T_1AM-treated mice. The result shows significant difference between control and treated hearts (*indicates $P = 0.008$, $n = 3$). Error bars: SEM; P values were obtained from two-tailed Student's t-test. (A color version of this figure is available in the online journal)

which may be consistent with its ability to induce hypothermia *in vivo*.[1]

This study revealed increase versus decrease of the OS level in the mitochondrial respiratory chain of kidney versus heart from the T_1AM treated mice as compared to corresponding control untreated tissues. The maximum projection images (Figure 1, right vs. left panels) show that in the high dose T_1AM-treated kidneys, the NADH concentration is lower (darker image) and the FAD concentration is higher (brighter image) as compared to those of kidneys from control mice, indicating a significant decrease in the NADH RR in kidneys from the high dose T_1AM treated versus the control tissue. The significant difference in the mean values of NADH RR of the two histograms in Figure 1 shows a significant increase, 19% ($\pm$ 0.4), in the OS level in kidneys from the high dose T_1AM-treated mice.

Moreover, the maximum projection images in Figure 2 demonstrate that the NADH concentration in the low dose and high dose T_1AM treated hearts is higher (brighter image) and the FAD concentration is lower (darker image) than those of control hearts. These changes signify an increase in the NADH RR of both low dose- and high dose-treated hearts versus control hearts, indicating less OS in the heart which is consistent with the previously reported protective role of T_1AM in this tissue.[32,33] The difference in the mean values of the red and green histograms as compared to the blue histogram (Figure 2) indicates a lower oxidation state in the high than in the low dose T_1AM-treated hearts (14% vs. 9% decrease as compared with controls).

Our results show consistent dose dependent effects of T_1AM in the mitochondrial redox state in heart and kidneys. These changes include a 19% ($\pm$0.4) decrease in the mean value of NADH RR of the high dose treated kidneys and 14% ($\pm$0.5) increase in the mean NADH RR of the high dose-treated hearts as compared to their appropriate controls, indicating that the NADH RR can be used as a reliable marker to quantify changes of the OS in tissues.

Our results suggest that T_1AM is a potent amine with a different physiological stimulation in the kidney versus heart. These differences may be related to different levels of T_1AM uptake in different tissues. Comparing the treated kidneys to the treated hearts, the change in the mean value of NADH RR is greater in kidneys, indicating a higher OS in this tissue than in the heart, consistent with higher accumulation of T_1AM in kidneys than in the heart.[24]

Previous studies showed that T_1AM treatment increased lipid breakdown and decreased lipid synthesis. Hence, excess lipid mobilization at high T_1AM concentration may also cause more OS in highly metabolically active organs such as kidney and liver.

Our assumption in this study is that changes in the mitochondrial pool of NADH are a key contributor to the measured changes in the NADH fluorescence signal. However, cytosolic NADH, nuclear NADH, and NADPH also contribute to the observed effects,[43] given that their fluorescence characteristics are the same as NADH. Chance et al. demonstrated that the fluorescence signal originates mostly from NADH in the mitochondria and the contribution of NADH—present in cytosol—is very small.[38] It has also shown that the concentration of NADH is about five times greater than NADPH; the NADH quantum yield is 1.25–2.5 times greater than NADPH, and metabolic perturbations only affect NADH.[39,40] Since cytosolic NADH and NADPH have been shown to fluoresce at levels much less intense than NADH, these contributions can be considered negligible.

Unlike NADH which has cytosolic and mitochondrial components, FAD are strictly localized within the mitochondria[41] and therefore the FAD signal derives only from the mitochondria.[42]

In conclusion, our results demonstrate quantitative capability of an optical cryoimaging technique to measure the tissue mitochondrial redox state in control or treated tissues. Our method is a direct analysis of the cellular metabolic state within the mitochondrial compartment of tissue. Here, we have applied our technique to the kidney and heart of low and high dose T_1AM-treated mice, which has not previously been reported. Our results show that treatment with T_1AM has a significant impact on the tissue-specific oxidative state of the mitochondria. Also, these data support the need for further study to discover the mechanism of action and metabolic pathways affected by T1AM, which may increase T1AM's potential as a future human weight loss drug.

Author Contributions: All authors participated in the interpretation of the studies and analysis of the data and review of the manuscript. HR, DEB and GC conducted T_1AM animal treatments. SM imaged the tissue and prepared the panels. ZG performed the statistical analysis and wrote the manuscript. AP and MR provided insights on data interpretation and provided the financial support for these studies.

ACKNOWLEDGEMENTS

The authors would like to acknowledge Whitney Wyatt Linz for helpful comments and for editing the manuscript. We acknowledge the support of RGI 7 (101x248) and NIH 8KL2TR000056 to MR and 1R01 DC009018, and RC4EY021357-01 to FAP.

REFERENCES

1. Scanlan TS, Suchland KL, Hart ME, Chiellini G, Huang Y, Kruzich PJ, Frascarelli S, Crossley DA, Bunzow JR, Ronca-Testoni S, Lin ET, Hatton D, Zucchi R, Grandy DK. 3-iodothyronamine is an endogenous and rapid-acting derivative of thyroid hormone. *Nat Med* 2004;**10**:638–42
2. Chiellini G, Frascarelli S, Ghelardoni S, Carnicelli V, Tobias SC, DeBarber A, Brogioni S, Ronca-Testoni S, Cerbai E, Grandy DK, Scanlan TS, Zucchi R. Cardiac effects of 3-iodothyronamine: a new aminergic system modulating cardiac function. *FASEB J* 2007;**21**:1597–608
3. Scanlan TS. Endogenous 3-Iodothyronamine (T(1)AM): more than we bargained for. *J Clin Endocrin Metab* 2011;**96**:1674–6
4. Braulke LJ, Klingenspor M, DeBarber A, Tobias SC, Grandy DK, Scanlan TS, Heldmaier G. 3-Iodothyronamine: a novel hormone controlling the balance between glucose and lipid utilisation. *J Comp Physiol B* 2008;**178**:167–77
5. Manni ME, De Siena G, Saba A, Marchini M, Landucci E, Gerace E, Zazzeri M, Musilli C, Pellegrini-Giampietro D, Matucci R, Zucchi R, Raimondi L. Pharmacological effects of 3-iodothyronamine (T1AM) in mice include facilitation of memory acquisition and retention and reduction of pain threshold. *Br J Pharmacol* 2013;**168**:354–62
6. Klieverik LP, Janssen SF, van Riel A, Foppen E, Bisschop PH, Serlie MJ, Boelen A, Ackermans MT, Sauerwein HP, Fliers E, Kalsbeek A. Thyroid hormone modulates glucose production via a sympathetic pathway from the hypothalamic paraventricular nucleus to the liver. *Proc Natl Acad Sci USA* 2009;**106**:5966–71
7. Galli E, Marchini M, Saba A, Berti S, Tonacchera M, Vitti P, Scanlan TS, Iervasi G, Zucchi R. Detection of 3-iodothyronamine in human patients: a preliminary study. *J Clin Endocrin Metab* 2012;**97**:E69–E74
8. Lodovici M, Bigagli E, Bardini G, Rotella CM. Lipoperoxidation and antioxidant capacity in patients with poorly controlled type 2 diabetes. *Toxicol Indus Health* 2009;**25**:337–41
9. Ramanujam N, Richards-Kortum R, Thomsen S, Mahadevan-Jansen A, Follen M, Chance B. Low temperature fluorescence imaging of freeze-trapped human cervical tissues. *Opt Express* 2001;**8**:335–43
10. Maleki S, Sepehr R, Staniszewski K, Sheibani N, Sorenson CM, Ranji M. Mitochondrial redox studies of oxidative stress in kidneys from diabetic mice. *Biomed Opt Express* 2012;**3**:273–81
11. Ranji M, Kanemoto S, Matsubara M, Grosso MA, Gorman JH 3rd, Gorman RC, Jaggard DL, Chance B. Fluorescence spectroscopy and imaging of myocardial apoptosis. *J Biomed Opt* 2006;**11**:064036
12. Ranji M, Matsubara M, Leshnower BG, Hinmon RH, Jaggard DL, Chance B, Gorman RC, Gorman Iii JH. Quantifying acute myocardial injury using ratiometric fluorometry. *IEEE Trans Biomed Eng* 2009;**56**:1556–63
13. Sepehr R, Staniszewski K, Maleki S, Jacobs ER, Audi S, Ranji M. Optical imaging of tissue mitochondrial redox state in intact rat lungs in two models of pulmonary oxidative stress. *J Biomed Opt* 2012;**17**:046010
14. Chance B, Schoener B, Oshino R, Itshak F, Nakase Y. Oxidation-reduction ratio studies of mitochondria in freeze-trapped samples. NADH and flavoprotein fluorescence signals. *J Biol Chem* 1979;**254**:4764–71
15. Ranji M, Nioka S, Xu HN, Wu BH, Li LZ, Jaggard DL, Chance B. Fluorescent images of mitochondrial redox states in in situ mouse hypoxic ischemic intestines. *J Innov Opt Health Sci* 2009;**2**:365–74
16. Lewis KE, Chung RS, West AK, Chuah MI. Distribution of exogenous metallothionein following intraperitoneal and intramuscular injection of metallothionein-deficient mice. *Histol Histopathol* 2012;**27**:1459–70
17. Jiang CH, Wang XF, Yin B, Li XY, Cui XM. Effects of exogenous nitric oxide on the subcellular distribution and chemical forms of copper in tomato seedlings under copper stress. *Ying Yong Sheng Tai Xue Bao* 2012;**23**:3033–9
18. Zhang ZH, Blessington D, Li H, Busch TM, Glickson J, Luo QM, Chance B, Zheng G. Redox ratio of mitochondria as an indicator for the response of photodynamic therapy. *J Biomed Opt* 2004;**9**:772–8
19. Xu HN, Zhao H, Mir TA, Lee SC, Feng M, Choe R, Glickson JD, Li LZ. Chop therapy induced mitochondrial redox state alteration in non-Hodgkin's lymphoma xenografts. *J Innov Opt Health Sci* 2013;**6**:1350011
20. Ostrander JH, McMahon CM, Lem S, Millon SR, Brown JQ, Seewaldt VL, Ramanujam N. Optical redox ratio differentiates breast cancer cell lines based on estrogen receptor status. *Cancer Res* 2010;**70**:4759–66
21. Li LZ, Xu HN, Ranji M, Nioka S, Chance B. Mitochondrial redox imaging for cancer diagnostic and therapeutic studies. *J Innov Opt Health Sci* 2009;**2**:325–41
22. Maleki S, Sepehr R, Staniszewski K, Sheibani N, Sorenson CM, Ranji M. Mitochondrial redox studies of oxidative stress in kidneys from diabetic mice. *Biomed Opt Express* 2012;**3**:273–81
23. Ranji M, Jaggard DL, Apreleva SV, Vinogradov SA, Chance B. Simultaneous fluorometry and phosphorometry of Langendorff perfused rat heart: ex vivo animal studies. *Opt Lett* 2006;**31**:2995–7
24. Matsubara M, Ranji M, Leshnower BG, Noma M, Ratcliffe SJ, Chance B, Gorman RC, Gorman JH 3rd. In vivo fluorometric assessment of cyclosporine on mitochondrial function during myocardial ischemia and reperfusion. *Ann Thorac Surg* 2010;**89**:1532–7
25. Chiellini G, Erba P, Carnicelli V, Manfredi C, Frascarelli S, Ghelardoni S, Mariani G, Zucchi R. Distribution of exogenous [125I]-3-iodothyronamine in mouse in vivo: relationship with trace amine-associated receptors. *J Endocrinol* 2012;**213**:223–30
26. Maleki S, Gopalakrishnan S, Ghanian Z, Sepehr R, Schmitt H, Eells J, Ranji M. Optical imaging of mitochondrial redox state in rodent model of retinitis pigmentosa. *J Biomed Opt* 2013;**18**:16004
27. Green DRE, van GI. A matter of life and death. *Cancer Cell* 2002;**1**:19–30
28. Todaro M, Zeuner A, Stassi G. Role of apoptosis in autoimmunity. *J Clin Immunol* 2004;**24**:1–11
29. Fierabracci P, Pinchera A, Martinelli S, Scartabelli G, Salvetti G, Giannetti M, Pucci A, Galli G, Ricco I, Querci G, Rago T, Di Salvo C, Anselmino M, Vitti P, Santini F. Prevalence of endocrine diseases in

morbidly obese patients scheduled for bariatric surgery: beyond diabetes. *Obes Surg* 2011;**21**:54–60
30. Saba A, Chiellini G, Frascarelli S, Marchini M, Ghelardoni S, Raffaelli A, Tonacchera M, Vitti P, Scanlan TS, Zucchi R. Tissue distribution and cardiac metabolism of 3-iodothyronamine. *Endocrinology* 2010;**151**:5063–73
31. Hoefig CS, Kohrle J, Brabant G, Dixit K, Yap B, Strasburger CJ, Wu Z. Evidence for extrathyroidal formation of 3-iodothyronamine in humans as provided by a novel monoclonal antibody-based chemiluminescent serum immunoassay. *J Clin Endocrin Metab* 2011;**96**:1864–72
32. Frascarelli S, Ghelardoni S, Chiellini G, Galli E, Ronca F, Scanlan TS, Zucchi R. Cardioprotective effect of 3-iodothyronamine in perfused rat heart subjected to ischemia and reperfusion. *Cardiovasc Drug Ther* 2011;**25**:307–13
33. Watt IN, Montgomery MG, Runswick MJ, Leslie AGW, Walker JE. Bioenergetic cost of making an adenosine triphosphate molecule in animal mitochondria. *Proc Natl Acad Sci USA* 2010;**107**:16823–7
34. Cumero S, Fogolari F, Domenis R, Zucchi R, Mavelli I, Contessi S. Mitochondrial F0F1-ATP synthase is a molecular target of 3-iodothyronamine, an endogenous metabolite of thyroid hormone. *Brit J Pharmacol* 2012;**166**:2331–47
35. Goglia F, Lanni A, Horst C, Moreno M, Thoma R. In vitro binding of 3,5-di-iodo-L-thyronine to rat liver mitochondria. *J Mol Endocrinol* 1994;**13**:275–82
36. Lanni A, Moreno M, Cioffi M, Goglia F. Effect of 3,3′-di-iodothyronine and 3,5-di-iodothyronine on rat liver mitochondria. *J Endocrinol* 1993;**136**:59–64
37. Venditti P, Napolitano G, Di Stefano L, Chiellini G, Zucchi R, Scanlan TS, Di Meo S. Effects of the thyroid hormone derivatives 3-iodothyronamine and thyronamine on rat liver oxidative capacity. *Mol Cell Endocrinol* 2011;**341**:55–62
38. Chance B, Cohen P, Jobsis F, Schoener B. Intracellular oxidation-reduction states in vivo. *Science* 1962;**137**:499–508
39. Avi-Dor Y, Olson J, Doherty M, Kaplan N. Fluorescence of pyridine nucleotides in mitochondria. *Biol Chem* 1962;**237**:7
40. Klaidman LK, Leung AC, Adams JD Jr. High-performance liquid chromatography analysis of oxidized and reduced pyridine dinucleotides in specific brain regions. *Anal Biochem* 1995;**228**:312–7
41. Heikal AA. Intracellular coenzymes as natural biomarkers for metabolic activities and mitochondrial anomalies. *Biomark Med* 2010;**4**:241–63
42. Aldakkak M, Stowe DF, Lesnefsky EJ, Heisner JS, Chen Q, Camara AK. Modulation of mitochondrial bioenergetics in the isolated Guinea pig beating heart by potassium and lidocaine cardioplegia: implications for cardioprotection. *J Cardiovasc Pharmacol* 2009;**54**:298–309
43. Rocheleau JV, Head WS, Piston DW. Quantitative NAD(P)H/flavoprotein autofluorescence imaging reveals metabolic mechanisms of pancreatic islet pyruvate response. *J Biol Chem* 2004;**279**:31780–7

(Received April 30, 2013, Accepted September 27, 2013)